Effects of Silver Nanoparticles on Photoelectrochemical Responses of Organic Dyes†

Taichi Arakawa,‡ Takatoshi Munaoka,§ Tsuyoshi Akiyama,‡,∥ and Sunao Yamada*,‡,∥,⊥

Department of Materials Physics and Chemistry, Kyushu University, 744 Motooka, Nishi-ku, Fukuoka 819-0395, Japan, Department of Materials Science and Engineering, School of Engineering, Kyushu University, 744 Motooka, Nishi-ku, Fukuoka 819-0395, Japan, Department of Applied Chemistry, Kyushu University, 744 Motooka, Nishi-ku, Fukuoka 819-0395, Japan, and Center for Future Chemistry, Kyushu University, 744 Motooka, Nishi-ku, Fukuoka 819-0395, Japan

Received: February 28, 2009; Revised Manuscript Received: May 7, 2009

The electrostatic layer-by-layer adsorption technique was used to fabricate silver nanoparticle (AgP)−organic dye composite films on indium−tin−oxide (ITO) electrodes. The degree of immobilization for the AgPs on the ITO electrode could be controlled by changing the immersion time of the electrode in the AgP aqueous colloidal solution. Porphyrin and phthalocyanine were selected as the dye molecules here because the former has a strong absorption band around the plasmon band of isolated AgPs, while the latter has one around the plasmon band of aggregated AgPs (interparticle plasmon coupling). Remarkable enhancement in the photocurrent action and fluorescence excitation spectra was observed for both dyes when considerable amounts of AgPs were deposited onto the ITO electrode. The Raman scattering measurements suggested the effects of enhanced electric fields resulting from localized surface plasmon resonance and light scattering on the photocurrent enhancement.

Introduction

Studies on the photoelectrochemical responses of dyes in the excited state are very important for elucidating the nature of fundamental photochemical reactions such as photoinduced electron-transfer during photosynthesis.[1] They also have practical applications such as in the development of organic solar cells[2] and photoelectrochemical biosensing devices,[3] logic gates,[4] and photocatalysis.[5] In a previous study, the photoelectrochemical responses of organic dyes were enhanced by the combined use of electron donor−acceptor pairs.[6]

Meanwhile, metal nanoparticles (NPs) have attracted much attention for their unique optical properties and have been utilized to improve the efficiency of photoelectric conversion[7−29] in solid-state photodiodes,[7−12] photodetecters,[13−15] solar cells,[16−19] and so on. In these cases, however, NPs (or nanoislands) are prepared by vacuum deposition,[11−15,17,18,22−28] lithography,[19−21] or casting from a colloidal solution;[7−9,16] thus, controlling the density of the deposited NPs and maintaining uniform size and shape has been difficult. As an alternative approach, we fabricated photovoltaic systems by the self-assembly of organic dyes either on a gold nanoparticle (AuP) multistructure prepared by a salting-out process[30] or a gold nanoparticle film prepared at a liquid−liquid interface.[31] Those approaches, however, also suffered from a lack of control over the AuP deposition density.

Previously, we reported a technique for the electrostatic layer-by-layer adsorption of silver nanoparticles (AgPs) on substrates for fabricating multistructures.[32] This technique is very convenient and needs no sophisticated equipment such as vacuum systems. Nevertheless, the deposition density of charged metal nanoparticles is easily controlled by the changing the time for which the substrate is immersed in the corresponding colloidal solution.[33] Quite recently, we found remarkable enhancement in the photocurrent responses resulting from the photoexcitation of porphyrin adsorbed onto AgP surfaces instead of AuP; the AgP−porphyrin assemblies were prepared by the layer-by-layer technique.[34] However, the detailed mechanism responsible has not yet been elucidated.

In the present study, we extensively investigated the change in the properties of the photocurrent produced of organic dyes when adsorbed onto different amounts of AgPs by using fluorescence and Raman scattering spectroscopy along with photocurrent generation measurements. We also investigated the photoelectrochemical response of phthalocyanine, which has absorption bands in the far-red region, to show the versatility of the AgP film.

Experimental Section

Materials. Silver nitrate ($AgNO_3$, Wako), trisodium citrate dehydrate (Wako), 5,10,15,20-tetraphenyl-21*H*,23*H*-porphyrin (TPP; Wako), rhodamine 6G (R6G; Sigma-Aldrich), poly(ethyleneimine) (PEI, $M_w = 50\,000-100\,000$; Wako), poly(styrenesulfonate) (PSS, $M_w = 70\,000$, Aldrich), and other chemicals were used as received. Chloroauric acid was synthesized in our laboratory. Phthalocyanine derivative (Pc) was supplied by Mitsui Chemicals, Inc. Silver nanoparticles (AgPs) were synthesized according to the reported procedure.[32,35] In brief, $AgNO_3$ (90 mg) is dissolved into H_2O (500 mL). After refluxing, 10 mL of sodium citrate aqueous solution (10 wt %) is injected into the solution and then refluxed for 30 min to produce the AgP colloidal solution. The resultant AgPs are capped with citrate ions, leading to negatively charged surfaces. The average diameter of the AgPs was 40 ± 19 nm; this was determined from transmission electron microscope images. An indium−tin−oxide (ITO) electrode (Geomatec co., ltd.) was washed with acetone and ethanol and then cleaned in an ozone atmosphere

† Part of the "Hiroshi Masuhara Festschrift".
* To whom correspondence should be addressed.
‡ Department of Materials Physics and Chemistry.
§ Department of Materials Science and Engineering.
∥ Department of Applied Chemistry.
⊥ Center for Future Chemistry.

10.1021/jp9018525 CCC: $40.75
Published on Web 05/27/2009

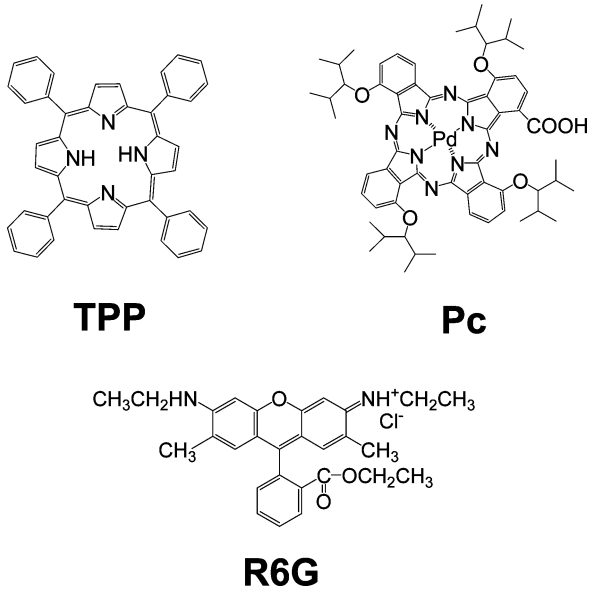

Figure 1. Structures of molecules.

for 15 min; this was followed by washing with H_2O and drying with the nitrogen gas before use.

Fabrication of AgP−Dye Films. The fabrication procedure for AgP−dye films with differing amounts of AgPs is shown in Figure 2. First, the ITO substrate was immersed in an aqueous PEI solution (45 mg/mL) containing 0.2 M NaCl for 20 min at 30 °C. Then, the substrate was immersed in an aqueous PSS solution (42 mg/mL) containing 0.2 M NaCl for 20 min at 30 °C to produce an ITO substrate modified with PEI and PSS (PSS/PEI/ITO). After the withdrawal in each step, the substrate was washed with H_2O and dried with nitrogen gas. Next, PSS/PEI/ITO was again immersed into the PEI solution, followed by washing with H_2O and drying with nitrogen gas; this formed a precursor-modified ITO substrate denoted as PEI/PSS/PEI/ITO;[32,36] hereafter, PEI/PSS/PEI is omitted. This positively charged ITO electrode was then immersed in an aqueous colloidal solution of negatively charged AgPs for different times (x = 0, 1, 4, 6, and 12 h) at 30 °C to electrostatically adsorb AgPs onto the positively charged ITO substrate (denoted as AgP(x)/ITO). Next, 5 μL of a toluene solution of TPP (0.1 mM) was spin-coated onto the surface of AgP(x)/ITO at 1500 and then 2000 rpm for 10 s each using a photoresist spinner (KYOWARIKEN K-359S-1); this produced the TPP-modified AgP(x)/ITO, which is denoted as TPP/AgP(x)/ITO. In a similar manner, 5 μL of a toluene solution of phthalocyanine derivative (Pc) (1 mM) was also spin-coated on the surface of AgP(x)/ITO, producing a Pc-modified AgP(x)/ITO denoted as Pc/AgP(x)/ITO (x = 0 or 12 h). The amount of adsorbed TPP or Pc on each substrate was evaluated from absorption spectroscopy. The adsorbed TPP or Pc was dissolved with toluene by immersing the dye-modified ITO electrode into toluene (5 mL for TPP and 10 mL for Pc); the electrode was then sonicated for 20 min.

Measurements. Absorption spectra were taken on a JASCO V-670 spectrophotometer. Scanning electron microscope (SEM) images were taken on a Hitachi S-5000. The sample was dried in a vacuum for over 6 h and platinum sputtering was carried out for 20 s before the SEM measurements. Photocurrent measurements were carried out in an aqueous solution containing 0.1 M $NaClO_4$ using the three-electrode photoelectrochemical cell; the three electrodes were modified (working), Ag/AgCl (sat. KCl), and platinum (counter). Before measurements, oxygen bubbling was carried out for 30 min. The monochromatic light from a Xe lamp irradiated the modified electrode, and the resultant photocurrents were measured with a Huso HECS-318C potentiostat. All photocurrents were measured at E = 0 V versus Ag/AgCl.

Fluorescence excitation spectra were taken using a JASCO FP-6600 spectrofluorometer. Raman spectra were analyzed using a JASCO NRS-1000N Raman spectrometer with a cooled CCD (DV401-FI-120, ANDOR TECHNOLOGY). The excitation light source was a He−Ne laser light (632.8 nm, GLG5731, Showa Optronics Co., Ltd.) through a bandpass filter. Samples for Raman scattering spectroscopy were prepared by dropping 200 μL of an ethanol solution of R6G (100 μM) onto AgP(x)/ITO, where an O-ring and cover glass were used to prevent vaporization of the ethanol (see the Supporting Information, Figure S1).

Results and Discussion

Characterization of AgP−Dye Films. Characterization of TPP/AgP(x)/ITO was carried out by absorption and SEM measurements. Figure 3a shows absorption spectra of TPP/AgP(x)/ITO, where x = 0, 1, 4, 6, and 12 h. The broad absorption band around 400−450 nm can be assigned to the plasmon band of isolated AgPs, or the band for the transverse oscillation mode of coupled particles; the broadband around 600−800 nm can be assigned to the plasmon band of AgP aggregates as well as the band for the longitudinal oscillation mode of coupled particles, as reported previously.[37] The weak absorption band around 420−440 nm can be assigned to the Soret band for TPP. It is slightly red-shifted compared to TPP in a toluene solution (419 nm). This may be attributed to the aggregation of TPP in TPP/AgP(x)/ITO or the electronic interaction between AgP and TPP; however, the reason why is not clear at this stage. In order to evaluate the amount of adsorbed TPP in TPP/AgP(x)/ITO, we dissolved the adsorbed TPP of TPP/AgP(x)/ITO by immersing it in toluene (see the Experimental Section). We found the Soret band of TPP in the absorption spectra of the TPP-containing toluene solution, as shown for TPP/AgP(12)/ITO in Figure 3b. The broad absorption spectrum of TPP-containing toluene solution may be based on the slight dissolution of AgPs having a plasmon band at around 410 nm into the toluene solution (see Figure 3b). Therefore, the adsorption spectrum of TPP-containing solution is the sum of the components of AgP and TPP. The results indicate the adsorption of TPP onto AgP(x)/ITO. From the intensity of Soret band, the average amount of adsorbed TPP in TPP/AgP(12)/ITO was calculated to be the 5.3×10^{13} molecules/cm^2. Despite the fact that the amounts of adsorbed TPP among TPP/AgP(x)/ITO (x = 0, 1, 4, 6, and 12 h) were somewhat different depending on the absorption spectroscopy, the difference fell within twice (see the Supporting Information, Figure S2).

Figure 4 shows SEM images of TPP/AgP(x)/ITO (x = 0, 1, 4, 6, and 12 h), where AgPs are indicated as white spots. It is clear that the number of AgPs increased; at the same time, aggregation proceeded as the immersion time (x) in the aqueous colloidal solution increased. These results indicate that the surface coverage can be controlled by changing the immersion time of the substrate in the colloidal solution.

Photoelectrochemical Measurements of AgP−TPP Films. In order to investigate the effects of AgPs on photocurrent responses from AgP−dye samples, we measured the photocurrent action spectra for all samples. The results for TPP/AgP(x)/ITO are shown in Figure 5; average data of three or four samples are shown. In all samples, photocurrents were observed in the

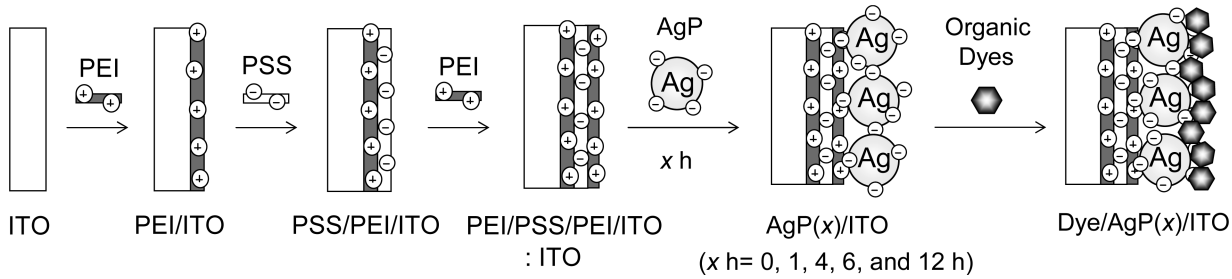

Figure 2. Schematic illustration for the fabrication of AgP−dye films on the ITO electrode.

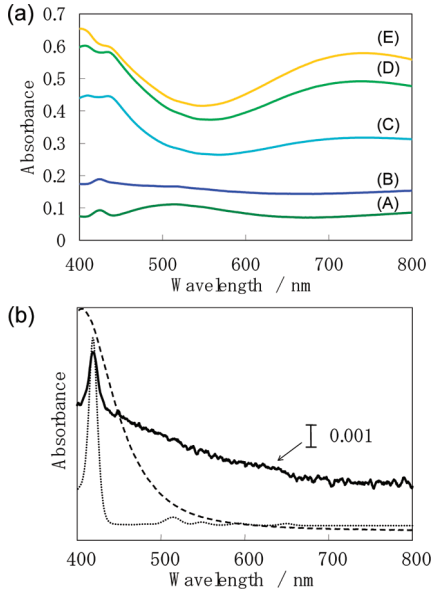

Figure 3. (a) Absorption spectra of TPP/AgP(x)/ITO, where x = (A) 0, (B) 1, (C) 4, (D) 6, and (E) 12 h. (b) Absorption spectrum of the toluene solution after dissolving the adsorbed TPP of TPP/AgP(12)/ITO (solid line), TPP in toluene (dotted lines), and silver colloidal solution (dashed line).

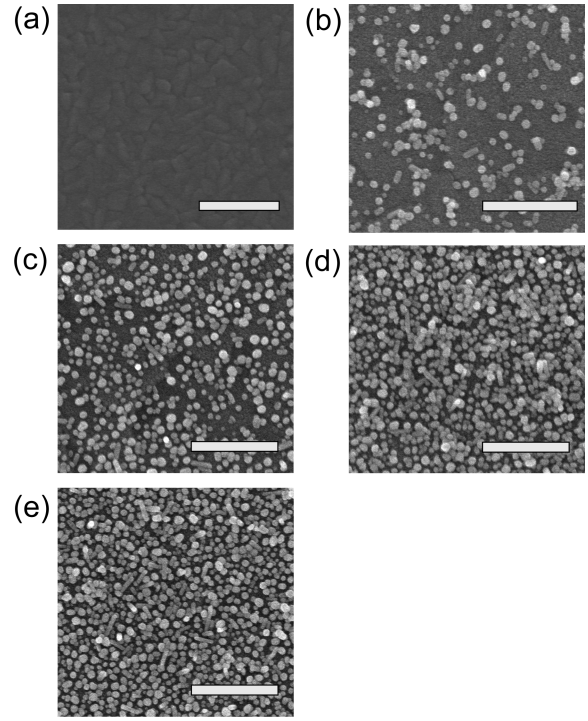

Figure 4. SEM images of TPP/AgP(x)/ITO, where x = (a) 0, (b) 1, (c) 4, (d) 6, and (e) 12 h. (scale bar = 500 nm).

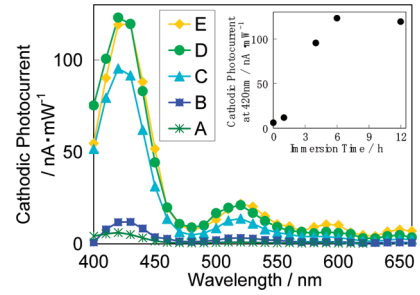

Figure 5. Photocurrent action spectra of TPP/AgP(x)/ITO, where x = (A) 0, (B) 1, (C) 4, (D) 6, and (E) 12 h; (inset) relationships between the photocurrent intensity at 420 nm and immersion time (x) for adsorption of AgPs on the ITO electrode.

cathodic direction except for AgP(x)/ITO; AgP(x)/ITO showed anodic photocurrent responses though the reason is not clear at this stage.[32] The photocurrent profiles of TPP/AgP(x)/ITO were correlated with the absorption spectrum of TPP in toluene. Therefore, it is suggested that the photocurrent response is initiated by photoexcitation of TPP and the subsequent electron-transfer to the oxygen in the electrolyte solution. It is noteworthy that the photocurrent increased as the immersion time (x) in the AgP aqueous colloidal solution increased i.e. increasing the adsorbed amount of AgPs; this is clearly shown in the inset of Figure 5. These results strongly suggest that the photoelectric conversion efficiency via the excited state of TPP depends on the surface coverage of AgPs. In particular, a 20- to 50-fold enhancement was observed for TPP/AgP(6)/TPP compared to TPP/AgP(0)/ITO. The photocurrent enhancement tended to saturate above an immersion time of 6 h. Since the incident light irradiates from the ITO side (reverse side to the TPP layer), most of the incident light is absorbed by AgPs before it reaches the TPP layer. Thus, the saturation profile of the photocurrent may be due to the decrease of light that can be absorbed by TPP; isolated AgPs preferentially absorb incident light around 420 nm.

Fluorescence Excitation and Raman Measurements of AgP−TPP Films. It has been known that the metal nanoparticles enhance the molecular fluorescence due to effects of localized surface plasmon resonance.[38] In order to find out the mechanism of the photocurrent enhancement shown in Figure 5, the fluorescence excitation and Raman scattering spectra were measured. Figure 6 shows the fluorescence excitation spectra of TPP/AgP(x)/ITO (x = 0, 1, 4, 6, and 12 h) monitored at 730 nm, where TPP/AgP(x)/ITO was irradiated from the front (direct irradiation of TPP layer) or rear (from the side of ITO electrode) sides (Figures 6, panels a and b, respectively); the spectra are shown as the average data of four samples. Also, the fluorescence excitation intensities at 420 and 550 nm were compared as functions of the immersion time (x) reflecting the amount of AgP adsorption onto the ITO electrode (Figure 4). In the front side geometry (Figure 6a), the fluorescence signal tended to

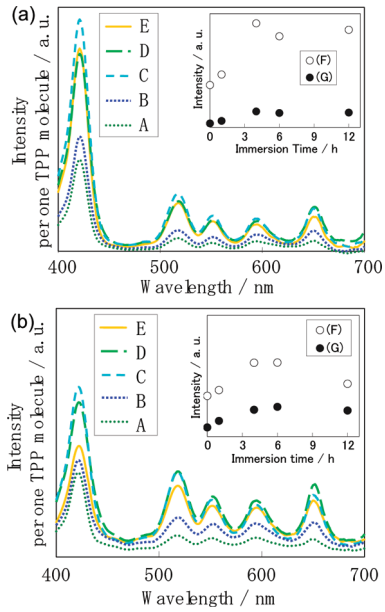

Figure 6. Fluorescence excitation spectra of TPP/AgP(x)/ITO, where x = (A) 0, (B) 1, (C) 4, (D) 6 and (E) 12 h. Irradiation direction of light: (a) front side (from TPP/AgP(x) film); (b) rear side (from ITO electrode); (inset) relationships between fluorescence signal at (F) 420 or (G) 550 nm and the immersion time (x) for adsorption of AgPs onto the ITO electrode.

saturate up to ~4 h. We also irradiated TPP/AgP(x)/ITO from the rear side (Figure 6b). In this case, the fluorescence signal at 420 nm increased up to 4 h of immersion time (x) and then decreased above 4 h. In contrast, the fluorescence signal at 550 nm increased up to ~6 h and then tended to saturate as in the cases (both 420 and 550 nm) for the front side geometry. These results strongly suggest that in the case of the rear side geometry, the increase in the amount of adsorbed AgPs led to a decrease in the incident light at 420 nm for excitation of the strong Soret band region; this led to a decrease in the fluorescence signal of TPP due to the so-called filter effect. Accordingly, it is suggested that the degrees of fluorescence enhancement with increasing the number of deposited AgPs are comparable between front- and rear side irradiation. The slight difference of the intensity profiles between photocurrent (Figure 5) and fluorescence excitation (Figure 6) is not clear at this stage.

It has also been well-known that surface-enhanced Raman scattering (SERS) profoundly depends on the localized electric fields caused by localized surface plasmon resonance.[39] Thus, we have investigated Raman scattering profiles of AgP(x)/ITO (see the Supporting Information, Figure S1). Raman scattering spectra of R6G adsorbed onto AgP(x)/ITO (x = 0, 1, 4, 6, and 12 h) are shown in Figure 7. The clear peaks at 1181, 1308, 1362, 1509, 1568, and 1645 cm^{-1} come from R6G, as reported previously.[39] These signals increased not monotonically with the immersion time (x) up to 4 h and tended to saturate above 4 h. This intensity profile suggests the contribution of SERS and correlates with the profiles of photocurrent action (Figure 5) and fluorescence excitation (Figure 6) spectra. These results demonstrate that dyes in the vicinity of AgP(x) with large x can receive strong electromagnetic fields generated by localized surface plasmon resonance as well as the effects of light scattering. On the other hand, the photocurrent generation mechanism is as follows. First, TPP is photoexcited and then the oxidized TPP is generated by photoinduced electron-transfer reaction to oxygen in the electrolyte solution. Next, the ITO electrode supplies the electron to the oxidized TPP. Accordingly,

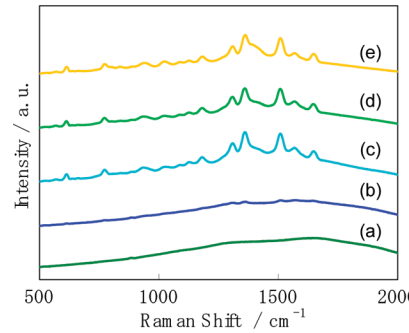

Figure 7. Raman scattering spectra of R6G deposited on AgP(x)/ITO, where x = (a) 0, (b) 1, (c) 4, (d) 6, and (e) 12 h.

cathodic photocurrent is observed. From the results of fluorescence enhancement for TPP (Figure 6), it is strongly suggested that the excited state of TPP leading to photoinduced electron-transfer reaction is also increased. At the same time, the scattered light must also contribute to the photocurrent enhancement at least some extent, though quantitative evaluation is difficult at this stage. It is not clear at this stage why the photocurrent, fluorescence, and Raman signals tend to show similar saturation profiles. One of the plausible reasons is the aggregation of AgPs. As the immersion time increases, the deposited AgPs tend to aggregate randomly, as shown in Figure 4. The strength and spot number of the enhanced electric fields become very complicated. Thus, it is suggested that the overall enhancement of the electric field in the measurement region does not necessarily increase, despite an increase in the number of deposited AgPs. We should also consider the possibility of aggregation of TPPs. As can be seen in Figure 6, fluorescence excitation spectra of TPP/AgP(x)/ITO are well correlated with the absorption spectrum of TPP in solution. In addition, the coverage of TPP on the ITO electrode was the order of monolayer level. These aspects suggest that the aggregation of TPP is less occurring in this case.

The effects of light scattering in TPP/AgP(x)/ITO were investigated by synchronous spectral measurements. The ratios of scattering signals of TPP/AgP(x)/ITO (x = 1, 4, 6 and 12) as compared with that of TPP/AgP(0)/ITO (without AgPs) are at most 3−6 times (TPP/AgP(4)/ITO showed exceptionally larger values: 3−9 times). On the other hand, the degree of photocurrent enhancement was 20−50 times (vide supra), roughly 1 order of magnitude different from the scattering results. Accordingly, it is suggested that the localized electric fields significantly influence for the photocurrent enhancement, though the effects of scattered light also should be taken into consideration.

Versatility of Polyion−AgP Films. Since the plasmon bands of AgP(x)/ITO appear in visible (400−450 nm) and far-red (600−800 nm) regions (Figure 3(a)), we also investigated the effects of localized electric fields caused by the plasmon band of the far-red region for coupled plasmon bands; we used Pc showing strong absorption bands in the 600−800 nm region. The results for the photocurrent measurements of Pc/AgP(x)/ITO (x = 0 and 12 h) are shown in Figure 8a. In this case, the amount of adsorbed Pc were comparable (to within ± 20%). The action spectra were correlated with the absorption spectrum of Pc in toluene, and the photocurrents were observed in the cathodic direction as in the case of TPP/AgP(x)/ITO. Therefore, it is suggested that the photocurrent responses can also be attributed to the photoexcitation of Pc followed by electron-transfer to oxygen. The broadening of the photocurrent peak may be attributed to the difference in environment or aggregation

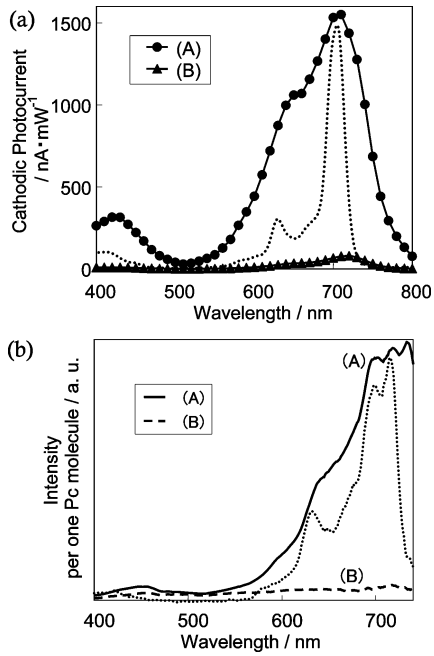

Figure 8. (a) Photocurrent action and (b) fluorescence excitation spectra of Pc/AgP(x)/ITO, where x = (A) 12 and (B) 0 h. The dotted line in (a) shows the absorption spectrum of Pc in toluene. The dotted line in (b) shows the fluorescence excitation spectrum of Pc in toluene.

of Pc in Pc/AgP(12)/ITO. An enormous photocurrent enhancement in Pc/AgP(12)/ITO as compared to Pc/AgP(0)/ITO can definitely be seen (typically more than 20 times at 710 nm). The fluorescence excitation spectra for Pc/AgP(x)/ITO (x = 0 and 12 h) monitored at 770 nm are shown in Figure 8b. Each profile is correlated to the fluorescence excitation spectrum of Pc in toluene; therefore, the excited species in each sample is Pc. Moreover, the excitation efficiency of Pc in Pc/AgP(12)/ITO is clearly enhanced 17 times at 710 nm compared to Pc/AgP(0)/ITO in terms of photocurrent signals (Figure 8a). These results suggest that photocurrent enhancement in Pc/AgP(12)/ITO should be attributed to the enhancement of Pc excitation efficiency caused by the enhanced electric field and light scattering. The results also suggest that the present polyion−AgP film effectively functions as the electrode that can induce not only fluorescence enhancement but also photocurrent enhancement in the wavelength region from the visible to far-red region independent of the dye species.

Conclusions

We verified the remarkable enhancement of molecular excitation in the presence of AgPs with diameters of 40 ± 19 nm. The degree of molecular excitation is strongly dependent on the number of deposited AgPs on the ITO electrode through electrostatic layer-by-layer adsorption with polyions. From the comparison of fluorescence, Raman scattering, and photocurrent signals, we verified that the localized electric fields appearing at the surface region of deposited AgPs and light scattering contribute to the enhancement of molecular excitation, which leads to larger fluorescence and photocurrent signals compared to without AgPs. These results suggest that the polyion−AgP electrode fabricated by the layer-by-layer technique is a promising approach for customized, highly efficient, and versatile photoelectric conversion systems and emission devices.

Acknowledgment. This work was supported by Research Fellowships of the Japan Society for Promotion of Science (JSPS) for Young Scientists (HAG0002126) and by a Grant-in-Aid for Young Scientists (A) (18685023), and on Priority Area (Area code 470, Strong Photon-Molecule Coupling Fields: No. 19049012) from the Ministry of Education, Culture, Sports, Science and Technology of Japan. The authors thank Mr. T. Kawahara and Mr. S. Matsumura for the SEM measurements.

Supporting Information Available: Experimental setup for the measurement of the SERS spectra of R6G adsorbed on AgP(x)/ITO and the amount of adsorbed TPP in the TPP/AgP(x)/ITO, where x = 0, 1, 4, 6, and 12 h. This material is available free of charge via the Internet at http://pubs.acs.org.

References and Notes

(1) (a) Das, R.; Kiley, P. J.; Segal, M.; Norville, J.; Yu, A. A.; Wang, L.; Trammell, S. A.; Reddick, L. E.; Kumar, R.; Stellacci, F.; Lebedev, N.; Schnur, J.; Bruce, B. D.; Zhang, S.; Baldo, M. *Nano. Lett.* **2004**, *4*, 1079. (b) Frolov, L.; Rosenwaks, Y.; Carmeli, C.; Carmeli, I. *Adv. Mater.* **2005**, *17*, 2434. (c) Lu, Y.; Xu, J.; Liu, Y.; Liu, B.; Xu, C.; Zhao, D.; Kong, J. *Chem. Commun.* **2006**, 785.

(2) (a) O'Regan, B.; Grätzel, M. *Nature* **1991**, *353*, 737. (b) Obermeyer, P.; Haase, C.; Stiebig, H. *Appl. Phys. Lett.* **2008**, *92*, 181102.

(3) (a) Ogasawara, S.; Ikeda, A.; Kikuchi, J. *Chem. Mater.* **2006**, *18*, 5982. (b) Okamoto, A.; Kamei, T.; Saito, I. *J. Am. Chem. Soc.* **2006**, *128*, 658. (c) Liang, M.; Liu, S.; Wei, M.; Guo, L.-H. *Anal. Chem.* **2006**, *78*, 621.

(4) (a) Nitahara, S.; Akiyama, T.; Inoue, S.; Yamada, S. *J. Phys. Chem. B* **2005**, *109*, 3944. (b) Matsui, J.; Mitsuishi, M.; Aoki, A.; Miyashita, T. *Angew. Chem., Int. Ed.* **2003**, *42*, 2272. (c) Gill, R.; Patolsky, F.; Katz, E.; Willner, I. *Angew. Chem., Int. Ed.* **2005**, *44*, 4554.

(5) (a) Fujishima, A.; Honda, K. *Nature* **1972**, *238*, 37. (b) Emeline, A. V.; Furubayashi, Y.; Zhang, X.; Jin, M.; Murakami, T.; Fujishima, A. *J. Phys. Chem. B* **2005**, *109*, 24441. (c) Izawa, K.; Yamada, T.; Unal, U.; Ida, S.; Altuntasoglu, O.; Koinuma, M.; Matsumoto, Y. *J. Phys. Chem. B* **2006**, *110*, 4645.

(6) (a) Yamada, S.; Kohrogi, H.; Matsuo, T. *Chem. Lett.* **1995**, *24*, 639. (b) Dreuw, A.; Worth, G. A.; Cederbaum, L. S.; Head-Gordon, M. *J. Phys. Chem. B* **2004**, *108*, 19049. (c) Luo, C.; Guldi, D. M.; Imahori, H.; Tamaki, K.; Sakata, Y. *J. Am. Chem. Soc.* **2000**, *122*, 6535. (d) Terasaki, N.; Akiyama, T.; Yamada, S. *Langmuir* **2002**, *18*, 8666.

(7) Schaadt, D. M.; Feng, B.; Yu, E. T. *Appl. Phys. Lett.* **2005**, *86*, 063106.

(8) Sundararajan, S. P.; Grady, N. K.; Mirin, N.; Halas, N. J. *Nano Lett.* **2008**, *8*, 624.

(9) Lim, S. H.; Mar, W.; Matheu, P.; Derkacs, D.; Yu, E. T. *J. Appl. Phys.* **2007**, *101*, 104309.

(10) Konda, R. B.; Mundle, R.; Mustafa, H.; Bamiduro, O.; Pradhan, A. K.; Roy, U. N.; Cui, Y.; Burger, A. *Appl. Phys. Lett.* **2007**, *91*, 191111.

(11) Kwon, M.-K.; Kim, J.-Y.; Kim, B.-H.; Park, I.-K.; Cho, C.-Y.; Byeon, C. C.; Park, S.-J. *Adv. Mater.* **2008**, *20*, 1253.

(12) Pillai, S.; Catchpole, K. R.; Trupke, T.; Zhang, G.; Zhao, J.; Green, M. A. *Appl. Phys. Lett.* **2006**, *88*, 161102.

(13) Stuart, H. R.; Hall, D. G. *Appl. Phys. Lett.* **1998**, *73*, 3815.

(14) Collin, S.; Pardo, F.; Pelouard, J.-L. *Appl. Phys. Lett.* **2003**, *83*, 1521.

(15) Tang, L.; Miller, D. A. B.; Okyay, A. K.; Matteo, J. A.; Yuen, Y.; Saraswat, K. C.; Hesselink, L. *Opt. Lett.* **2006**, *31*, 1519.

(16) Derkacs, D.; Lim, S. H.; Matheu, P.; Mar, W.; Yu, E. T. *Appl. Phys. Lett.* **2006**, *89*, 093103.

(17) Pillai, S.; Catchpole, K. R.; Trupke, T.; Green, M. A. *J. Appl. Phys.* **2007**, *101*, 093105.

(18) Stuart, H. R.; Hall, D. G. *Appl. Phys. Lett.* **1996**, *69*, 2327.

(19) Hägglund, C.; Zäch, M.; Petersson, G.; Kasemo, B. *Appl. Phys. Lett.* **2008**, *92*, 053110.

(20) Reilly, T. H.; Lagemaat, J.; Tenent, R. C.; Morfa, A. J.; Rowlen, K. L. *Appl. Phys. Lett.* **2008**, *92*, 243304.

(21) Tvingstedt, K.; Persson, N.-K.; Inganäs, O. *Appl. Phys. Lett.* **2007**, *91*, 113514.

(22) Stenzel, O.; Stendal, A.; Voigtsberger, K.; Borczyskowski, C. *Sol. Energy Mater. Sol. Cells* **1995**, *37*, 337.

(23) Wen, C.; Ishikawa, K.; Kishima, M.; Yamada, K. *Sol. Energy Mater. Sol. Cells* **2000**, *61*, 339.

(24) Westphalen, M.; Kreibig, U.; Rostalski, J.; Lüth, H.; Meissner, D. *Sol. Energy Mater. Sol. Cells* **2000**, *61*, 97.

(25) Uemura, S.; Yoshida, M.; Kodzasa, T.; Yase, K.; Kamata, T. *Synth. Mat.* **2003**, *137*, 1443.

(26) Ishikawa, K.; Wen, C.-J.; Yamada, K.; Okubo, T. *J. Chem. Eng. Jpn.* **2004**, *37*, 645.

(27) Rand, B. P.; Peumans, P.; Forrest, S. R. *J. Appl. Phys.* **2004**, *96*, 7519.

(28) Morfa, A. J.; Rowlen, K. L.; Reilly, T. H.; Romero, M. J.; van de Lagemaat, J. *Appl. Phys. Lett.* **2008**, *92*, 013504.

(29) Kim, S.-S.; Na, S.-I.; Jo, J.; Kim, D.-Y.; Nah, Y.-C. *Appl. Phys. Lett.* **2008**, *93*, 073307.

(30) (a) Kuwahara, Y.; Akiyama, T.; Yamada, S. *Langmuir* **2001**, *17*, 5714. (b) Akiyama, T.; Inoue, K.; Kuwahara, Y.; Terasaki, N.; Niidome, Y.; Yamada, S. *J. Electroanal. Chem.* **2003**, *550*−*551*, 303. (c) Akiyama, T.; Inoue, K.; Kuwahara, Y.; Niidome, Y.; Terasaki, N.; Nitahara, S.; Yamada, S. *Langmuir* **2005**, *21*, 793.

(31) Akiyama, T.; Nakada, M.; Terasaki, N.; Yamada, S. *Chem. Commun.* **2006**, 395.

(32) Arakawa, T.; Akiyama, T.; Yamada, S. *Trans. Mater. Res. Soc. Jpn.* **2008**, *33*, 185.

(33) (a) Gole, A.; Sainkar, S. R.; Sastry, M. *Chem. Mater.* **2000**, *12*, 1234. (b) Yonezawa, T.; Onoue, S.; Kunitake, T. *Adv. Mater.* **1998**, *10*, 414.

(34) Arakawa, T.; Munaoka, T.; Akiyama, T.; Yamada, S. *in preparation*.

(35) Lee, P. C.; Meisel, D. *J. Phys. Chem.* **1982**, *86*, 3391.

(36) Schmitt, J.; Decher, G.; Dressick, W. J.; Brandow, S. L.; Geer, R. E.; Shashidhar, R.; Calvert, J. M. *Adv. Mater.* **1997**, *9*, 61.

(37) Goulet, P. J. G.; dos Santos, D. S.; Alvarez-Puebla, R. A.; Oliveira, O. N.; Aroca, R. F. *Langmuir* **2005**, *21*, 5576.

(38) (a) Kulakovich, O.; Strekal, N.; Yaroshevich, A.; Maskevich, S.; Gaponenko, S.; Nabiev, I.; Woggon, U.; Artemyev, M. *Nano. Lett.* **2002**, *2*, 1449. (b) Akiyama, T.; Kawahara, T.; Arakawa, T.; Yamada, S. *Jpn. J. Appl. Phys.* **2008**, *47*, 3063. (c) Tanaka, H.; Mitsuishi, M.; Miyashita, T. *Chem. Lett.* **2005**, *34*, 1246.

(39) (a) Nie, S.; Emory, S. R. *Science* **1997**, *275*, 1102. (b) Michaels, A. M.; Jiang, J.; Brus, L. *J. Phys. Chem. B* **2000**, *104*, 11965. (c) Emory, S. R.; Haskins, W. E.; Nie, S. *J. Am. Chem. Soc.* **1998**, *120*, 8009. (d) Suzuki, M.; Niidome, Y.; Kuwahara, Y.; Terasaki, N.; Inoue, K.; Yamada, S. *J. Phys. Chem. B* **2004**, *108*, 11660.

JP9018525